A three-dimensional breakdown model of SOI lateral power transistors with a circular layout*

Guo Yufeng(郭宇锋)[1, 2, †], Wang Zhigong(王志功)[1], and Sheu Gene(许健)[3]

(1 Institute of RF- & OE-ICs, Southeast University, Nanjing 210096, China)
(2 Nanjing University of Posts and Telecommunications, Nanjing 210003, China)
(3 Department of Computer Science & Information Engineering, Asia University, Taichung, Taiwan, China)

Abstract: This paper presents an analytical three-dimensional breakdown model of SOI lateral power devices with a circular layout. The Poisson equation is solved in cylindrical coordinates to obtain the radial surface potential and electric field distributions for both fully- and partially-depleted drift regions. The breakdown voltages for N^+N and P^+N junctions are derived and employed to investigate the impact of cathode region curvature. A modified RESURF criterion is proposed to provide a design guideline for optimizing the breakdown voltage and doping concentration in the drift region in three dimensional space. The analytical results agree well with MEDICI simulation results and experimental data from earlier publications.

Key words: SOI; three dimensional; breakdown voltage; model; RESURF
DOI: 10.1088/1674-4926/30/11/114006 **PACC:** 7340Q; 7340T

1. Introduction

SOI high voltage ICs have been developed for power applications due to such properties as perfect isolation, fast switching, high integration density and low power consumption. As a key component in SOI power ICs, SOI power devices with a circular layout are frequently utilized to maximize performance and minimize device area[1−4]. 2-D/3-D TCAD simulations are effective tools to help understand the underlying physics and optimize the geometry of SOI lateral power devices. To complement these numerical tools, an exact analytical model is a powerful tool to investigate the operating mechanism of SOI power devices quantitatively and develop design schemes. Many 1-D and 2-D analytical models have been developed to predict the electric field distribution and breakdown voltage of SOI lateral power devices[5−8]. However, these models are incapable of describing the three dimensional effect of the circular layout such as electric field crowding due to the curvature of the drain region. In practice, taking 3-D effects into account is important to optimize the device parameters and improve the operating performance[9].

In this paper, we report a 3-D analytical model for SOI lateral power devices that considers the influence of the curvature of the cathode/drain region. 3-D Poisson equations in the drift region are solved. The analytical expressions for the surface potential, electric fields, and breakdown voltage are derived for both completely and incompletely depleted cases. Numerical simulations and experimental data are employed to verify the model. Finally, we present a modified RESURF condition including the 3-D effect as a design guideline for SOI power devices.

2. Analytical model

A cross section of the SOI power device for modeling and simulation is shown in Fig. 1. The cylindrical coordinate system is chosen to have its origin on the r-axis at the surface of the top-Si layer and on the y-axis at the center of the drain region along the vertical direction.

When a large voltage $V_{\rm app}$ is applied at the cathode electrode while the anode electrode and substrate are grounded, the drift region is fully depleted and the electrostatic potential $\varphi(r, y)$ in the drift region satisfies the Poisson equations taking the following form:

$$\frac{\partial^2\varphi(r,y)}{\partial r^2}+\frac{1}{r}\frac{\partial\varphi(r,y)}{\partial r}+\frac{\partial^2\varphi(r,y)}{\partial y^2}=-\frac{qN_{\rm d}}{\varepsilon_{\rm s}}, \qquad (1)$$

where q is the electric charge, $\varepsilon_{\rm s}$ is the dielectric constant for Si, and $N_{\rm d}$ is the doping concentration in the drift region.

The second-order Taylor series expansion along the y dimension is employed to approximate the electrostatic potential in the depletion region:

$$\varphi(r,y)=\varphi(r,0)+\left.\frac{\partial\varphi(r,y)}{\partial y}\right|_{y=0}y+\left.\frac{\partial^2\varphi(r,y)}{\partial y^2}\right|_{y=0}\frac{y^2}{2}. \qquad (2)$$

Taking into account the Neumann boundary conditions between the field/buried oxide and the top-Si layer, we obtain

$$\left.\frac{\partial\varphi(r,y)}{\partial y}\right|_{y=0}=0, \quad \frac{\varphi(r,t_{\rm s})}{t_{\rm ox}}=-K\left.\frac{\partial\varphi(r,y)}{\partial r}\right|_{r=t_{\rm s}}, \qquad (3)$$

---

* Project supported by the National Natural Science Foundation of China (No. 60806027), the China Postdoctoral Science Foundation (No. 20070411013), the Natural Science Foundation of Jiangsu Province, China (No. BK2007605), and the State Key Laboratory of Electronic Thin Films and Integrated Devices (No. KF2007001).

† Corresponding author. Email: yfguo@njupt.edu.cn

Received 14 May 2009, revised manuscript received 3 July 2009

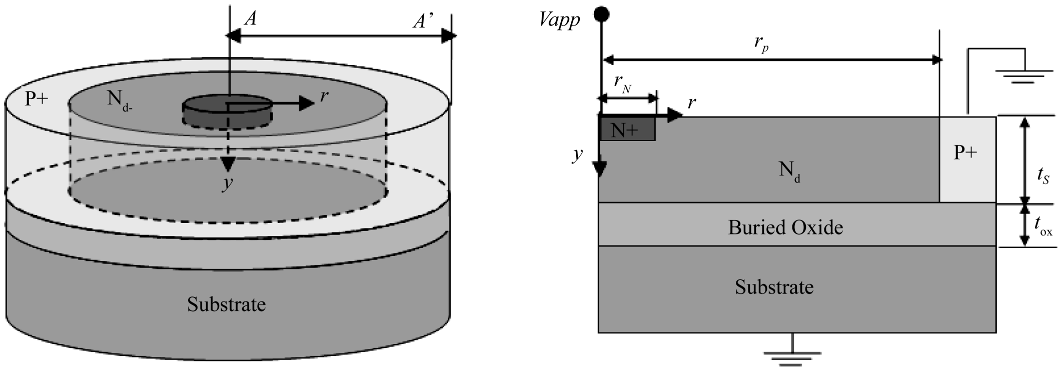

Fig. 1. SOI power diode with a circular layout: (a) 3-D device structure; (b) Cross section along the A-A' direction.

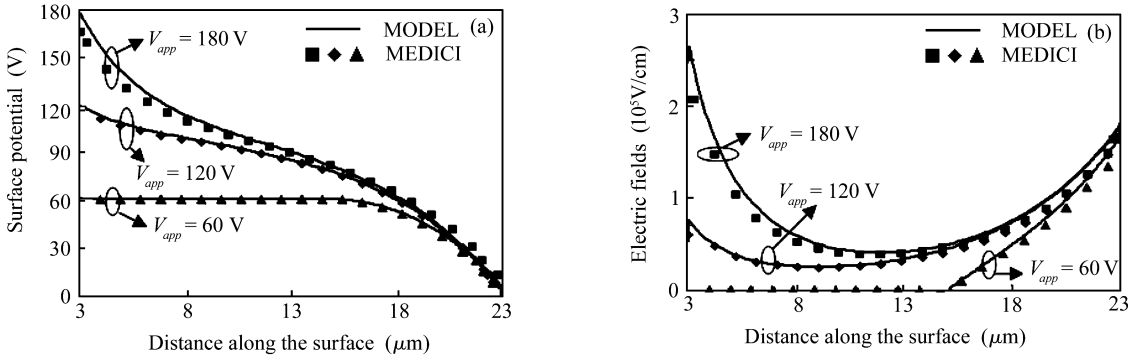

Fig. 2. Comparison of the analytical and numerical results for SOI RESURF devices with a radius of N^+ region curvature of 3 μm: (a) Surface potential distributions; (b) electric field distributions (t_s = 3 μm, t_{ox} = 2.5 μm, L_d = 20 μm, $N_d = 2.5 \times 10^{15}$ cm^{-3}).

where K is the dielectric constant ratio of Si to SiO_2.

Substituting Eqs. (2) and (3) into Eq. (1), a differential equation that describes the surface electrostatic potential can be derived:

$$\frac{\partial^2\varphi(r,0)}{\partial r^2}+\frac{1}{r}\frac{\partial\varphi(r,0)}{\partial r}+\frac{\varphi(r,0)}{t^2}=-\frac{qN_d}{\varepsilon_s}, \tag{4}$$

where t denotes characteristic thickness and is expressed as:

$$t=\sqrt{0.5t_s^2+Kt_st_{ox}}. \tag{5}$$

Neglecting the built-in potential of N^+N and P^+N junctions, we get the boundary condition:

$$\varphi(r_P,0)=0 \text{ and } \varphi(r_N,0)=V_{app}, \tag{6}$$

where r_N and r_P are the curvature of the N^+ region and the inner curvature of the P^+ region, respectively.

Solving Eq. (4) constrained by Eq. (6), we can express the surface potential and electric field distributions as follows:

$$\varphi(r,0)=\frac{(V_{app}-V_0)F_0(r/t,r_P/t)-V_0F_0(r_N/t,r/t)}{F_0(r_N/t,r_P/t)}+V_0, \tag{7}$$

$$E_r(r,0)=\frac{(V_{app}-V_0)F_1(r_P/t,r/t)+V_0F_1(r_N/t,r/t)}{tF_0(r_N/t,r_P/t)}, \tag{8}$$

where $V_0=qN_dt^2/\varepsilon_s$, $F_v(x,y)$ is the function:

$$F_v(x,y)=(-1)^vI_0(x)K_v(y)-K_0(x)I_v(y), \tag{9}$$

where $I_v(a)$ and $K_v(a)(v=0{,}1)$ are the modified Bessel functions of the first and second kinds about a, respectively.

For RESURF devices, lateral breakdown always occurs at the surface of N^+N and P^+N junctions. A useful parameter for identifying the onset of avalanche breakdown within device structures is the critical electric field[10]. Hereby, the breakdown voltages of lateral breakdown can be derived by substituting Eq. (8) into $E_r(r_N,0)=E_C^{NN}$ and $E_r(r_P,0)=E_C^{PN}$, where E_C^{NN} and E_C^{PN} are the critical electric fields when breakdown occurs at N^+N and P^+N junctions, respectively. Then

$$V_{BL}^{NN}=E_C^{NN}t\frac{F_0(r_N/t,r_P/t)}{F_1(r_P/t,r_N/t)}+V_0\left[\frac{t/r_N}{F_1(r_P/t,r_N/t)}+1\right], \tag{10}$$

$$V_{BL}^{PN}=V_0\left[1+\frac{r_P}{t}F_1(r_N/t,r_P/t)\right]-E_C^{PN}r_pF_0(r_N/t,r_P/t). \tag{11}$$

Equation (7)–(11) can be used to investigate the electrostatic potential, electric field, and breakdown voltage in a completely depleted drift region. For a lower applied voltage, however, the edge of the lateral depletion region does not reach the N^+N junction and the drift region is not completely depleted. In this case, the curvature of the N^+ region r_N in Eqs. (7)–(11) is replaced by the curvature of the lateral depletion region r_D, which can be computed by solving the following equation:

$$(r_D/t)\,F_1(r_P/t,r_D/t)-\frac{1}{V_{app}/V_0-1}=0. \tag{12}$$

3. Results and discussion

To verify the proposed analytical model, numerical simulations were performed using MEDICI in cylindrical coordinates. Figures 2 and 3 show the surface potentials and electric

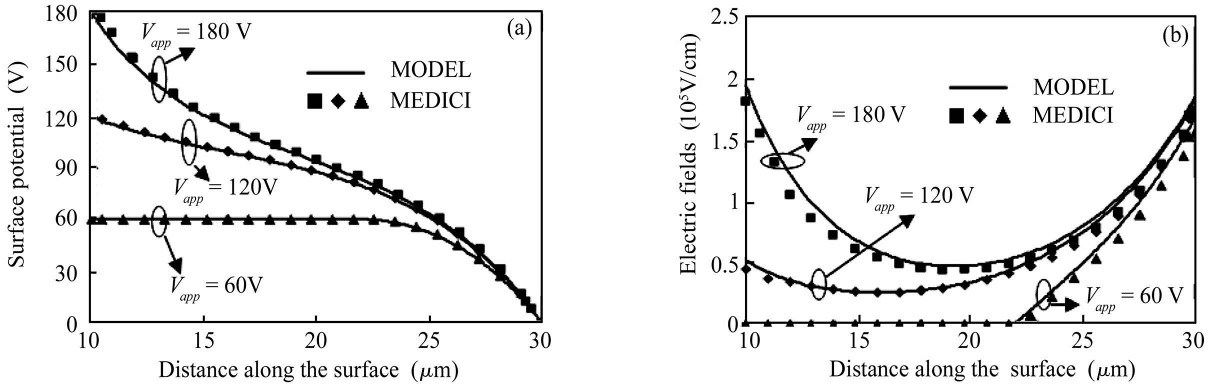

Fig. 3. Comparison of the analytical and numerical results for SOI RESURF devices with a radius of N$^+$ region curvature of 10 μm: (a) Surface potential distributions; (b) Electric field distributions (t_s = 3 μm, t_{ox} = 2.5 μm, L_d = 20 μm, N_d = 2.5 × 10^{15} cm^{-3}).

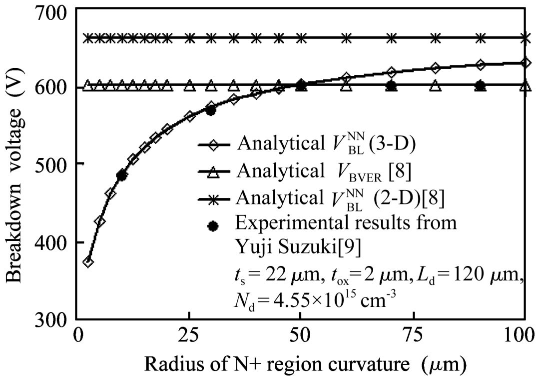

Fig. 4. Breakdown voltages as a function of the radius of N$^+$ region curvature.

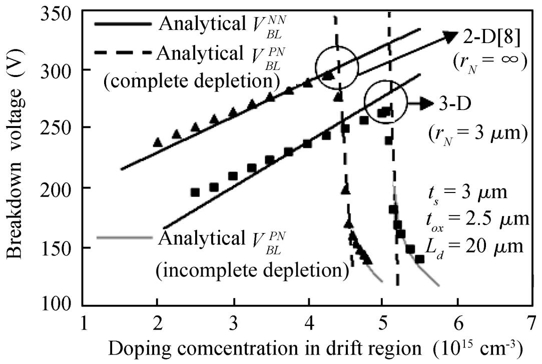

Fig. 5. Breakdown voltages as a function of doping concentration in the drift region.

field distributions of the SOI RESURF device for the different radii of cathode region curvatures. The square-, rhombus- and triangle-dot curves are the simulation results with various applied voltages, respectively. The solid curves are the analytical results of the proposed model. A fair agreement between the modeling and numerical results shows that the proposed model can be applied in the partial- and complete-depletion cases. Furthermore, when the radius of the cathode region curvature reduces from 10 to 3 μm, Figures 2(b) and 3(b) indicate that the maximum electric field at the cathode/drift junctions increases from 1.9 × 10^5 to 2.5 × 10^5 V/cm for the same applied voltage of 180 V. Such a crowding of the electric field due to the smaller curvature of the N$^+$ region usually lead to a lower breakdown voltage.

Figure 4 illustrates the breakdown voltage as a function of the radius of the N$^+$ region curvature. For reference, experimental results from previous publications and simulation results from MEDICI are also shown in the figure. As shown in Fig. 4(a), a smaller radius of curvature causes severe surface electric field crowding at the edge of the N$^+$N junction and thus results in a reduced breakdown voltage. With a larger radius of curvature, the release of the electric field crowding leads to a higher breakdown voltage up to a limit. Analytical results show that the maximum achievable breakdown voltage is determined by the vertical breakdown on the top-Si/buried-SiO$_2$ interface when the radius of the N$^+$N junction curvature exceeds 50 μm.

Figure 5 illustrates the impact of the doping concentration in the drift region on the breakdown voltage for both the 2-D and 3-D cases. The analytical 2-D breakdown voltages are calculated using the equations from our previous work[8]. The numerical and analytical results show that the 3-D breakdown voltages of the discussed devices are about 50% higher than the 2-D case for a lightly-doped drift region (under 4 × 10^{15} cm^{-3}). However, for a drift doping concentration between 4 × 10^{15} and 5 × 10^{15} cm^{-3}, the drift region of the 2-D structure is partial depleted when breakdown occurs, which results in a sharp decrease of breakdown voltage. In the 3-D structure, in contrast, the electric field crowding at N$^+$N junction still makes the drift region fully-depleted when breakdown occurs, and thus increasing breakdown voltages are exhibited. For a further increase of drift doping concentration (over 5 × 10^{15} cm^{-3}), very low breakdown voltages can be observed in Fig. 5 for both the 2-D and 3-D structures. This is because the very heavy doping concentration causes an incompletely-depleted drift region and thus a deteriorated voltage-sustaining capability along the lateral direction.

Theoretically, using the condition of $V_{BL}^{NN} = V_{BL}^{PN}$ and Eqs. (10), (11), we derive a modified RESURF criterion considering the 3-D effect of N$^+$ region curvature as follows:

$$N_d t \leqslant \alpha \frac{\varepsilon_s E_C}{q} \tag{13}$$

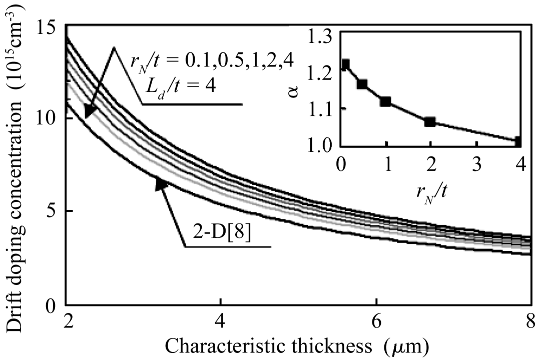

Fig. 6. Optimal drift doping concentration as a function of the characteristic thickness.

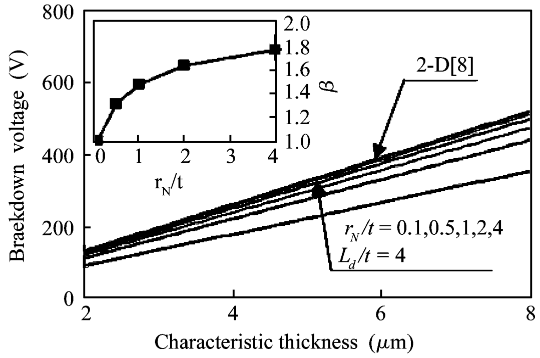

Fig. 7. Maximal breakdown voltage as a function of the characteristic thickness.

with

$$\alpha = \frac{F_0(r_\mathrm{N}/t, r_\mathrm{P}/t)\,[F_1(r_\mathrm{P}/t, r_\mathrm{N}/t) + t/r_\mathrm{P}]}{F_1(r_\mathrm{N}/t, r_\mathrm{P}/t)F_1(r_\mathrm{P}/t, r_\mathrm{N}/t) - t^2/\,(r_\mathrm{N}r_\mathrm{P})}. \qquad (14)$$

Further, the maximum breakdown voltage is expressed as:

$$V_\mathrm{B}^{\max} = \beta V_0 \leqslant \alpha\beta E_\mathrm{C} t \qquad (15)$$

with

$$\beta = 1 + \frac{F_1(r_\mathrm{N}/t, r_\mathrm{P}/t) + t/r_\mathrm{N}}{F_1(r_\mathrm{P}/t, r_\mathrm{N}/t) + t/r_\mathrm{P}}. \qquad (16)$$

Figures 6 and 7 show the maximal breakdown voltage and optimal drift doping concentration as functions of the characteristic thickness t, as well as the impacts of N^+ region curvature on α and β. Figure 6 indicates that α increases from 1 to 1.2 with reduction of the N^+ region curvature. Therefore, the optimal doping concentration in drift region should increase by 20% when considering the 3-D effect, which brings a positive effect to reduce the specific on-resistance. However, Figure 7 shows that β decreases sharply by 50% due to reduction of the N^+ region curvature. As a result, the breakdown voltage decreases by 40% compared to the 2-D situation. Therefore, we can strike a balance between breakdown voltage and on-resistance by optimizing the radius of the cathode region curvature in the design of SOI power devices.

4. Conclusions

An analytical breakdown model is proposed to predict the 3-D effect of the curvature of the cathode/drain region on the breakdown voltage of SOI lateral power devices. First, based on solving the 3-D Poisson equation in cylindrical coordinates, the surface electrostatic potential and electric field distributions are expressed as a compound Bessel function for both the partially and completely depleted conditions. Then, the breakdown voltages of the cathode/drift and anode/drift junctions are derived as a function of structure parameters. The model provides a quantitative description of the electric field crowding effect at the edge of the N^+ region, and also shows that a small radius of curvature leads to a reduced breakdown voltage as well as an increasing drift doping concentration, which is helpful in reducing specific on-resistance. Finally, a modified RESURF criterion for maximizing the breakdown voltage and minimizing the drift region resistance is proposed as a design scheme. The accuracy of the model is verified by numeral simulation results and published experimental data.

References

[1] Hidalgo S, Fernandez J, Godignon P, et al. Power lateral DMOS transistor test structures. Proc ICMTS Conf, 1993: 33

[2] Luo Xiaorong, Zhang Bo, Li Zhaoji, et al. A novel 700-V SOI LDMOS with double-sided trench. IEEE Electron Device Lett, 2007, 28(5): 422

[3] Guo Yufeng, Li Zhaoji, Zhang Bo. A new analytical model for optimizing SOI LDMOS with step doped drift region. Microelectron J, 2006, 37: 861

[4] Guo Yufeng, Li Zhaoji, Zhang Bo, et al. Fabrication of a novel SOI material with non-planar buried oxide layer. Chinese Journal of Semiconductors, 2007, 28(9): 1415

[5] Chung S K, Han S Y. Analytical model for the surface field distribution of SOI RESURF device. IEEE Trans Electron Devices, 1998, 45(6):1374

[6] Li W H, Luo J S. A novel analytical physical model for thin film SOI RESURF structure based on 2-D Poisson equation. Proc ISPSD, 1998: 724

[7] Merchant S. Analytical model for the electric field distribution in SOI RESURF and TMBS structures. IEEE Trans Electron Devices, 1999, 46(6): 1264

[8] Guo Yufeng, Li Zhaoji, Zhang Bo. A new two dimensional analytical breakdown model of SOI RESURF devices. Proc ICCCAS, 2007: 1278

[9] Suzuki Y, Kishida T, Takano H, et al. 3-D effect of cell designs on the breakdown voltage of power SOI-LDMOS. Proc IEEE Inter SOI Conf, 1996:134

[10] Baliga B J. Power semiconductor devices. Boston: International Thomson Publishing, 1996